Electron scattering from excited states in ^{14}N and ^{9}Be†

N. Ensslin,* W. Bertozzi, S. Kowalski, C. P. Sargent, W. Turchinetz, and C. F. Williamson
Laboratory for Nuclear Science and Department of Physics, Massachusetts Institute of Technology, Cambridge, Massachusetts 02139

and

S. P. Fivozinsky, J. W. Lightbody, Jr., and S. Penner
National Bureau of Standards, Washington, D.C. 20234

(Received 4 September 1973)

Electron scattering form factors have been measured for the first six excited states in ^{14}N and for the 2.429-MeV ($\frac{5}{2}^-$) level in ^{9}Be. The form factors for the lowest $T=1$ level in ^{14}N along with the previously measured ground-state magnetic moment are used to specify the $T=0$ and $T=1$ wave functions for the mass-14 system assuming two p-shell valence particles in an LS-coupling basis. The amplitudes of the various configurations so derived are generally in poor agreement with previous determinations, although the present wave functions yield values of the lifetime of the first $T=0$ state in ^{14}N and of the ^{14}N ground-state quadrupole moment that are in excellent agreement with previous measurements. The present data are not sufficiently precise to allow a direct separation of the $T=0$ and $T=1$ components for the first four negative-parity excited states. However, for two of these states which are excited primarily by $C1$ transitions, a comparison of the radiative strengths determined in this experiment with previous lifetime measurements sets a lower limit of 2% for the $T=1$ admixture.

[NUCLEAR REACTIONS ^{14}N (e,e'); measured form factors for first six excited levels; deduced wave functions for first $T=0$ and $T=1$ levels in mass 14; ^{9}Be (e,e'); measured form factors for 2.429-MeV level.]

I. INTRODUCTION

This paper describes the results of inelastic scattering from low-lying levels in ^{14}N and ^{9}Be over the momentum transfer range of 0.61 to 1.15 fm^{-1}. The level structure for ^{14}N is shown schematically in Fig. 1. Studied in the present experiment were the 2.313-MeV ($J=0^+$, $T=1$), 3.945-MeV ($J=1^+$, $T=0$), 4.913-MeV ($J=0^-$, $T=0$), 5.106-MeV ($J=2^-$, $T=0$), 5.69-MeV ($J=1^-$, $T=0$), and 5.83-MeV ($J=3^-$, $T=0$) levels in ^{14}N.

Historically the mass-14 nuclei have provided an important test of the presence of tensor forces. The β decay of ^{14}C to ^{14}N proceeds with the unusually long lifetime of 5690 years ($\log ft=9.03$). This transition is formally allowed, but it is hindered by a factor of 10^5 with respect to other Gamow-Teller transitions. There appears to be no reasonable explanation for this other than accidental cancellation of the β decay matrix element. This in turn requires either very strong configuration mixing or the inclusion of a tensor force in the nuclear interaction. Configuration mixing has been advocated by Inglis,[1] Baranger and Meshkov,[2] and Weidenmüller.[3] Calculations with a tensor force have been carried out by Jancovici and Talmi,[4] Elliot,[5] Visscher and Ferrell,[6] and Zamick.[7] Recently Rose, Häusser, and Warburton[8] reviewed this problem and concluded that a consistent fit of all γ- and β-decay matrix element of mass 14 cannot be achieved by configuration mixing alone but requires a tensor force.

Bishop, Bernheim, and Kossanyi-Demay[9] pointed out that the strength of the tensor force can be found by measuring the electron scattering cross sections for the 2.313(0^+) level in ^{14}N. In particular, the results of the present experiment can be used as a constraint on possible ^{14}N and ^{14}C ground-state wave functions.

The low-lying levels in ^{14}N have been studied by Bishop, Bernheim, and Kossanyi-Demay[9] by inelastic electron scattering. However, the resolution available to these workers did not allow separation of the negative-parity doublets at about 5.0 and 5.8 MeV, and poor statistical accuracy was obtained for the 2.313-MeV ($T=1$) level. The improved resolution now available at the National Bureau of Standards electron linear accelerator made possible for the first time the separation of all these levels and their study with reasonably good statistical accuracy.

II. EXPERIMENTAL ARRANGEMENT

This experiment was carried out at the electron linear accelerator facility of the National Bureau of Standards.[10] The accelerator was operated at energies between 60 and 120 MeV, and scattering angles of 110, 145, and 163° were employed. With 47- or 74-mg/cm^2-thick targets oriented in the transmission mode, the resolution of the system was about 0.10%. Average beam currents of 1–2 μA were used in the present experiment. The beam current was monitored by a Faraday cup located downstream from the target chamber and by a nonintercepting toroidal ferrite monitor[11] located upstream from the target chamber.

Sintered wafers of Be_3N_2 of 47- and 74-mg/cm^2 thickness were used as targets. With these targets it was possible to work at high resolution in the transmission mode without metallic windows or cooling devices necessary for gas or liquid targets. However, this choice of target required that additional beam time be devoted to provide data from a ^{9}Be target. Also, carbon and oxygen were present in 1% and 3% contaminations, respectively, and their effects had to be subtracted in analyzing the data.

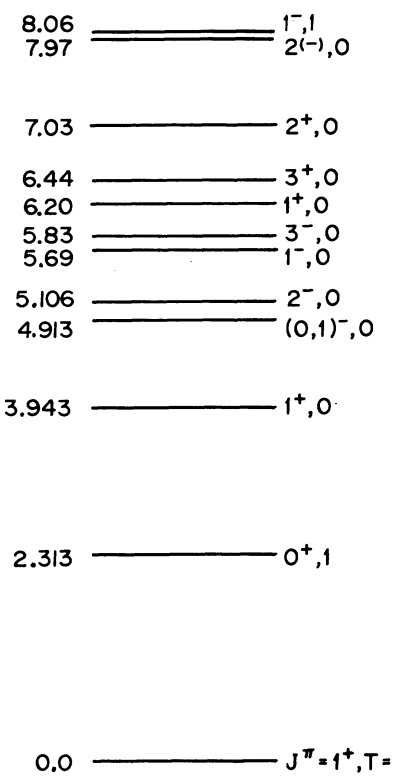

FIG. 1. Energy level diagram for ^{14}N.

The scattered electrons were analyzed by a 169.7° double-focusing ($n=\frac{1}{2}$) spectrometer having a 76-cm radius of curvature.[12] The scattered electrons were detected in the focal plane of the spectrometer by an array of 20 lithium-drifted silicon semiconductors[13] covering a momentum range of 1.4%. Two large plastic scintillators (12.7 cm × 10.2 cm × 0.3 cm) were situated directly behind this array. A triple coincidence requirement between the plastic scintillators and the semiconductors was used to reduce background events. Single counts in the 20 detectors, single counts and double coincidences in the plastic scintillators, triple coincidences, and other related data were collected by an on-line computer for display and later analysis.[14,15]

The data were also corrected for the relative efficiencies of the detectors. These were determined by moving the detector array along the focal plane in steps such that the detector positions were systematically overlapped. The ratio of the counts received by two adjacent detectors when one was moved to the position of the other was taken to be the ratio of their efficiencies.

III. DATA REDUCTION

A. Determination of peak areas

The raw data were corrected for dead-time and chance counting effects in the detection system. These corrections were straightforward and never exceeded 10%, typically amounting to about 3%. After the triple coincidences in each of the 20 detectors had been corrected for count-rate limitations and detector efficiencies, they were sorted into energy spectra of predetermined bin widths.

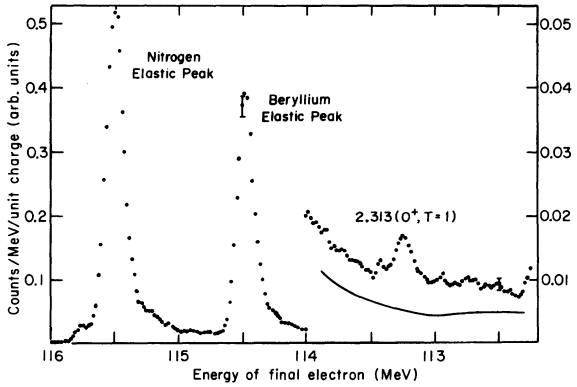

FIG. 2. Spectrum of 117.6-MeV electrons scattered at 145.6° from a 47-mg/cm^2 Be_3N_2 target. Small ^{16}O and ^{12}C peaks are visible just above and below the ^{14}N elastic peak. The solid line represents the amount of the tail due to ^{9}Be, as determined by normalized ^{9}Be data taken concurrently.

Two such spectra are illustrated in Figs. 2 and 3(a).

Properly normalized ^{9}Be spectra were next subtracted from the beryllium nitride spectra. The radiation tails of the elastic and inelastic peaks were then subtracted. These radiation tails were obtained in first Born approximation.[16,17] Included were the effects of bremsstrahlung and ionization losses in the target. Also included at this stage of the analysis was a constant room background and an energy-dependent background (between 0 and 10% of the radiation tail)[18,19] due to scattering within the spectrometer. In Fig. 3(b) this total background function is compared with the nitrogen inelastic spectrum of Fig. 3(a).

After background subtraction the areas of the elastic and inelastic peaks were determined by fitting to the data a shape that accounted for (a) radiative processes coherent with the scattering event, (b) Landau straggling and incoherent bremsstrahlung, and (c) the **resolution function** of the spectrometer-beam transport system (assumed Gaussian).[17] Contributions from scattering to excited states of the ^{12}C and ^{16}O contaminants were also included in the fitting procedure.

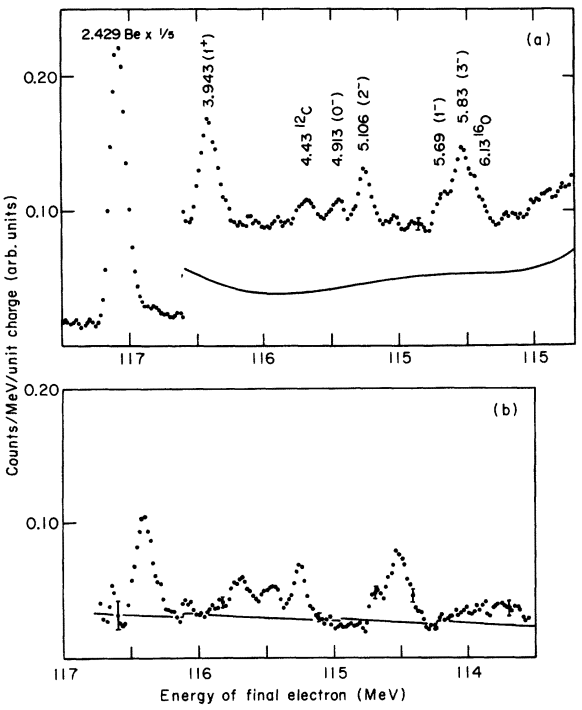

FIG. 3. (a) Spectrum of 122-MeV electrons scattered at 110.5° from a 74-mg/cm^2 Be_3N_2 target. Displayed is the excitation region from 3–6 MeV below the ^{14}N elastic peak with the corresponding smoothed ^{9}Be background shown as a solid line. (b) Spectrum with ^{9}Be contribution subtracted. The total background shape discussed in the text has been superimposed. Discontinuities in the background function are not physical, but symbolize the fact that the radiation tails of all inelastic peaks have been considered.

B. Error analysis

In addition to the usual statistical uncertainties, poorly resolved peaks were subject to errors correlated to the heights, widths, and positions of their nearby neighbors. These uncertainties were determined by varying the widths or positions of neighboring peaks and allowing the heights to readjust to a new best fit. The result was an approximately parabolic plot of χ^2 as a function of each of these parameters. For a nonlinear least-squares fit, the value of χ^2 which corresponds to an error of one standard deviation in one of the parameters is given by[20]

$$\chi^2(1\sigma) = \chi^2_{\min}\left[1 + \frac{F(1, N-p, 0.683)}{N-p}\right], \qquad (1)$$

where N is the number of data points used in the fit, p is the number of parameters varied in the fitting, $\chi^2_{\min}$ is the minimum χ^2 obtained in the fit, $F(\nu_1, \nu_2, r)$ is the statistical F distribution, ν_1 is the number of degrees of freedom in the numerator, ν_2 is the number of degrees of freedom in the denominator, and r is the confidence level. For $\nu_2 > 20$, $F(1, \nu_2, 0.683) \cong 1$. If $\chi^2_{\min}/\nu_2 \cong 1$ this reproduces the familiar "χ^2+1" rule.[21] For each peak the standard deviations correlated to position, width, and height were added linearly to the statistical standard deviation to arrive at the total standard deviation.

Possible error encountered from the background subtraction arises from two sources: (a) the statistical uncertainty in fitting the background function to the regions between the inelastic peaks, and (b) the uncertainty in choosing the form of the background function. Uncertainty (a) was calculated from Eq. (1) in the usual manner. Uncertainty (b) was estimated as follows: Several different "reasonable" background functions were used in the fitting procedure. Each function yielded slightly different values for the fitted parameters. The spread in these fitted values was taken as a measure of the relative uncertainty in choosing the background function. The uncertainty from source (a) was then combined in quadrature with the uncertainty from source (b) to obtain the total uncertainty due to background under the peak.

Systematic errors in the measured cross sections due to such experimental parameters as beam energy, spectrometer angle, spectrometer field calibration, detector position, and beam monitor calibration are believed to be of order

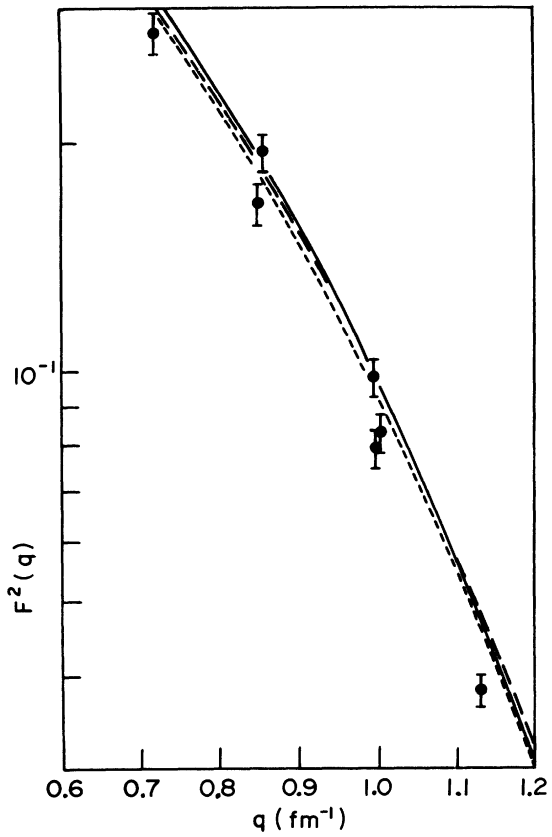

FIG. 4. ^{14}N elastic form factor squared. Best fits to the measurements of Ref. 9 (— —), Ref. 22 (---), and Ref. 23 (———) are compared. The results of Ref. 22 are fitted to the Coulomb monopole form factor only. The data points are elastic form factors obtained during the present experiment.

10^{-3} or less and have been neglected. Inelastic cross sections were measured relative to elastic cross sections so that many possible sources of experimental error cancel.

C. Calculation of form factors

Recent measurements of ^{14}N elastic scattering have been carried out by Bishop, Bernheim, and Kossanyi-Demay,[9] Dally, Croissiaux, and Schweitz,[22] and Bentz.[23] These results are plotted in Fig. 4 for the region of momentum transfer used in this experiment. Also shown are very approximate elastic cross sections obtained from the present experiment. These points serve only as a rough check on the measured target thickness and indicate that there are no large systematic errors. The ^{14}N elastic cross sections were instead obtained by a phase-shift calculation using the generalized harmonic-oscillator parameters $\alpha = 1.27$, $a = 1.70$ fm (corresponding to a root-mean-square radius R_m of 2.49 fm) obtained by Bentz.[23] These parameters were used because, although they were determined at low momentum transfers, they agreed well with the measurements of Dally, Croissiaux, and Schweitz[22] at the higher energies of this experiment. Where it was necessary to calculate ^{9}Be cross sections, the Bentz parameters ($\alpha = 0.62$, $a = 1.73$ fm, $R_m = 2.43$ fm) were again used.

Inelastic cross sections were then calculated from the relationship

$$\frac{d\sigma_i}{d\Omega} = \frac{d\sigma_0}{d\Omega}\frac{A_I}{A_E}, \tag{2}$$

where $d\sigma_i/d\Omega$ is the inelastic cross section, $d\sigma_0/d\Omega$ is the elastic cross section, A_I is the inelastic peak area, and A_E is the elastic peak area. Table I is a compilation of the calculated elastic and measured inelastic form factors.

The squared form factor is defined by

$$F^2(q) = \frac{d\sigma}{d\Omega} \Big/ \frac{d\sigma_M}{d\Omega}, \tag{3a}$$

$$\frac{d\sigma_M}{d\Omega} = \left(\frac{Z^2e^4}{4E_0^2}\right)\frac{\cos^2\frac{1}{2}\theta}{\sin^4\frac{1}{2}\theta}\,\frac{1}{1+(2E_0/M)\sin^2\frac{1}{2}\theta}, \tag{3b}$$

TABLE I. Elastic and inelastic form factors for ^{14}N.

Energy (MeV)	Angle (deg)	q [a] (fm^{-1})	$F^2(q)$ elastic (calculated)	$F^2(q)$ inelastic (measured) $\times 10^3$ 2.313 MeV	3.945 MeV	4.913 MeV	5.106 MeV	5.69 MeV	5.83 MeV
60.65	163.7	0.606	0.468	0.014 ± 0.002					
73.06	163.4	0.729	0.317	0.029 ± 0.003					
89.82	110.8	0.746	0.298		0.56 ± 0.02	0.10 ± 0.02	0.12 ± 0.01	0.06 ± 0.02	0.26 ± 0.03
86.31	163.4	0.860	0.191	0.037 ± 0.004					
90.08	145.9	0.868	0.185	0.038 ± 0.004	1.01 ± 0.13	0.17 ± 0.04	0.25 ± 0.05	0.14 ± 0.06	0.44 ± 0.07
104.95	110.8	0.871	0.184		0.85 ± 0.06	0.05 ± 0.3	0.30 ± 0.03	0.19 ± 0.04	0.47 ± 0.04
100.90	163.7	1.005	0.0970	0.044 ± 0.006					
104.62	145.7	1.006	0.0964	0.031 ± 0.004	$1.22^{+0.24}_{-0.12}$	0.25 ± 0.05	0.40 ± 0.05	0.29 ± 0.10	0.71 ± 0.11
122.00	110.5	1.010	0.0959		1.03 ± 0.10	0.25 ± 0.04	0.40 ± 0.04	0.28 ± 0.06	0.63 ± 0.06
117.62	145.7	1.130	0.0479	0.055 ± 0.004					
120.01	146.0	1.154	0.0412		0.87 ± 0.08	0.35 ± 0.04	0.50 ± 0.04	0.47 ± 0.06	0.92 ± 0.13

[a] Calculated for elastic scattering.

where $e^4=(\alpha\hbar c)^2$, α is the fine structure constant, Z is the atomic number of target, M is the rest mass of target (MeV), E_0 is the total energy of incident electron (MeV), and θ is the laboratory scattering angle. These form factors were interpreted within the framework of the first Born approximation in terms of longitudinal and transverse form factors

$$F^2(q)=F_c^{\,2}(q^2)+(\tfrac{1}{2}+\tan^2\tfrac{1}{2}\theta)F_T^{\,2}(q^2)\,, \tag{4}$$

where q is the momentum transferred by the electron to the nucleus (fm^{-1}), $F_c(q^2)$ is the longitudinal form factor, $F_T(q^2)$ is the transverse form factor. For the sake of comparison with transition strengths measured at $q=\omega$, where ω is the nuclear excitation energy, q was replaced by an "effective q" which corrects in an approximate way for the distortion of the electron wave by the Coulomb field of the nucleus[24];

$$q_{\rm eff}=q\left(1+\tfrac{3}{2}(\sqrt{\tfrac{3}{5}})^{1/2}\frac{Z\alpha}{E_0R_m}\right). \tag{5}$$

The transition strengths were then determined by extrapolating each multipole component of the form factors to $q=\omega$ and using the relations

$$B(CL,\omega)\uparrow=\frac{Z^2e^2}{4\pi}[(2L+1)!!]^2\,\frac{F_{CL}^{\,2}(\omega^2)}{\omega^{2L}}\,, \tag{6}$$

$$B(ML,\omega)\uparrow=\frac{Z^2e^2}{4\pi}\,\frac{L}{L+1}\,[(2L+1)!!]^2\,\frac{F_{ML}^{\,2}(\omega^2)}{\omega^{2L}}\,, \tag{7}$$

where L is the multipole order of the transition, $B(CL,\omega)\uparrow$ is transition strength for longitudinal excitation from the ground state, and $B(ML,\omega)\uparrow$ is transition strength for transverse magnetic excitation from the ground state. The corresponding single-particle units are

$$B_{\rm sp}(CL,\omega)\uparrow=\frac{1}{4\pi}\left(\frac{2J_f+1}{2J_0+1}\right)\left(\frac{3}{3+L}\right)^2 \times 1.2^{2L}A^{2L/3}e^2\ {\rm fm}^{2L}, \tag{8}$$

$$\left.\begin{matrix}B_{\rm sp}(ML,\omega)\uparrow\\ B_{\rm sp}(EL,\omega)\uparrow\end{matrix}\right\}=\frac{10}{\pi}\left(\frac{2J_f+1}{2J_0+1}\right)\left(\frac{3}{3+L}\right)^2 \times 1.2^{2L-2}A^{(2L-2)/3}\left\{\begin{matrix}\mu_0\\ e\end{matrix}\right\}^2{\rm fm}^{2L-2}\,, \tag{9}$$

where J_0 is intrinsic spin of the ground state, J_f is intrinsic spin of the excited state. All measured transition strengths are summarized in Table II.

IV. 2.313-MeV (0^+) ^{14}N LEVEL

A. Experimental observations

Figure 5 illustrates the 0^+ form factor as measured in this experiment and as reported earlier by Bishop, Bernheim, and Kossanyi-Demay.[9] At low momentum transfers the two measurements differ by nearly an order of magnitude. This difference is believed to be due to the fact that under the conditions of the earlier experiment the peak was very small and difficult to separate from the background. At higher q, the two experiments differ by only a factor of 2, almost within assigned errors. However, the form factors measured in the present experiment are systematically smaller than those of Ref. 9 for all of the excitations common to both experiments. The very rough elastic scattering form factors for ^{14}N as measured in the present experiments (Fig. 4) agree to within 10–15% with the elastic scattering data of Ref. 9. Also, the 2.429-MeV ^{9}Be form factors measured in this experiment are consistent with earlier results, as described in Sec. VII.

It is now believed[25] that the cross sections reported in Ref. 9 are too large for $q\leq 1.0$ fm^{-1} due to the very great difficulty of extracting the small peak from the background.

B. Theoretical interpretation

On the basis of their energies, spins, and parities, the 2.313-MeV first excited state of ^{14}N and the ground states of ^{14}C and ^{14}O are considered to be an isospin triplet. Except for Coulomb effects, the wave functions for all three states are expected to be identical. If it is assumed that there are two holes in the $1p$ shell and that there

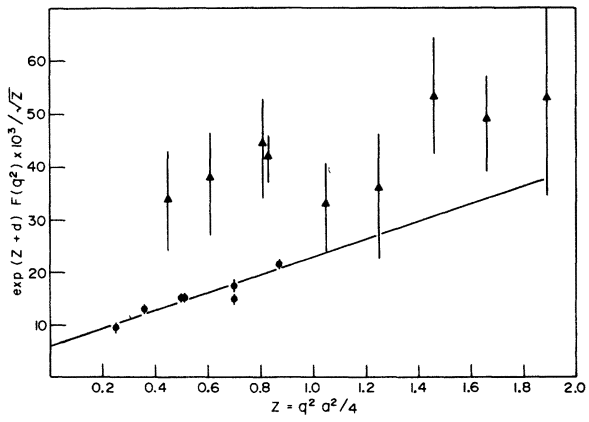

FIG. 5. Transverse magnetic form factors for the 2.313-MeV (0^+) level. The data of Ref. 9 are denoted by ▲, the present data by ●. The solid line is the fit to Eq. (16b).

TABLE II. Measured reduced transition probabilities.

Transition from ground state	Multipolarity L	$B(L,\omega)$† ($e^2\,\mathrm{fm}^{2L}$)	B/B_{sp}
$2.313(0^+)^{14}$N	$M1$	$(4.3 \pm 1.3)\times 10^{-30}$	0.065 ± 0.020
$3.945(1^+)^{14}$N	$C2$	3.40 ± 0.29	1.70 ± 0.14
$4.913(0^-)^{14}$N	$C1$	$(1.35 \pm 0.65)\times 10^{-8}$	$(1.1 \pm 0.5)\times 10^{-7}$
$5.106(2^-)^{14}$N	$C3$	80 ± 19	4.1 ± 1.0
$5.69(1^-)^{14}$N	$C1$	$(1.81 \pm 1.01)\times 10^{-8}$	$(3.8 \pm 2.1)\times 10^{-8}$
$5.83(3^-)^{14}$N	$C3$	166 ± 35	6.1 ± 1.3

are noncentral forces, the most general wave functions expressed in an LS-coupling basis are:

$$\psi(T=0) = \alpha\psi(^3S_1) + \beta\psi(^1P_1) + \gamma\psi(^3D_1), \tag{10}$$

$$\psi(T=1) = x\psi(^1S_0) + y\psi(^3P_0). \tag{11}$$

The following features of the mass-14 system can be expressed in terms of these wave functions:

(i) ^{14}C to ^{14}N ground-state β decay:

$$\langle f|\vec{\sigma}|i\rangle = \sqrt{6}\,(x\alpha - y\beta/\sqrt{3}) \cong 0, \tag{12}$$

where $\vec{\sigma}$ is the Gamow-Teller operator.

(ii) ^{14}N ground-state magnetic moment:

$$\mu = \tfrac{1}{2}(g_p + g_n)\alpha^2 + \tfrac{1}{2}\beta^2 + [\tfrac{3}{4} - \tfrac{1}{4}(g_p + g_n]\gamma^2, \tag{13}$$

where g_p is the g factor of the proton and g_n is the g factor of the neutron.

(iii) ^{14}N ground-state quadrupole moment:

$$Q = \frac{\langle r^2\rangle}{5}\left[\tfrac{4}{\sqrt{5}}\,\alpha\gamma - \beta^2 + \tfrac{7}{10}\,\gamma^2\right]. \tag{14}$$

(iv) 2.313-MeV ^{14}N to ground-state ^{14}N radiative lifetime:

$$T_m = \frac{6.49\times 10^{-15}\ \mathrm{sec}}{\{4.71(x\alpha - y\beta/\sqrt{3}) + [x\beta(2/3)^{1/2} - y\alpha(2/9)^{1/2} + y\gamma(5/18)^{1/2}]\}^2}\,. \tag{15}$$

(v) Electron scattering form factor for excitation of the 2.313-MeV state: For the single-particle shell model the multipole expansion of the form factors and the calculation of the radial integrals have been carried out by Willey[26] using harmonic-oscillator wave functions. For a pure $M1$ transition within the $1p$ shell the results are

$$F_{M1}(q^2) = \sqrt{z}\,[C_1\langle 1p|j_0(qr)|1p\rangle + C_2\langle 1p|j_2(qr)|1p\rangle]\,e^{-d},$$
$$= 0.0146[A_1\sqrt{z}\,(1 - \tfrac{2}{3}z) + B_1\sqrt{z}\,\tfrac{2}{3}z]\,e^{-(z+d)}, \tag{16a}$$

or

$$\frac{F_{M1}(q^2)}{\sqrt{z}\,e^{-(z+d)}} = 0.0146[A_1 + \tfrac{2}{3}(B_1 - A_1)z]. \tag{16b}$$

The factor e^{-d} corrects for the finite size of the proton and the lack of translational invariance of the shell-model wave function.[27] The symbols are defined as follows: a is the harmonic-oscillator parameter, $z = q^2a^2/4$, $d = q^2(a_p^2 - a^2/A)/4$, $a_p^2 = \frac{2}{3}$ (rms proton radius)^2 = 0.43 fm^2, and A is the atomic mass number of the target.

Results of the orbital and spin integrations, carried out with the formulas of DeForest and Walecka,[28] are

$$A_1 = 4.71\{x\alpha - y\beta/\sqrt{3}\} + \{x\beta(2/3)^{1/2} - y\alpha(2/9)^{1/2} + y\gamma(5/18)^{1/2}\}, \tag{17}$$

$$B_1 = 4.71\{x\gamma/\sqrt{5} + y\beta/2\sqrt{3} + y\gamma 3\sqrt{2}/4\sqrt{5}\} + \{x\beta(2/3)^{1/2} - y\alpha(2/9)^{1/2} + y\gamma(5/18)^{1/2}\}. \tag{18}$$

Exactly the same formulas were obtained by Peaslee[29] using different mathematical techniques.

The anomalously long lifetime of ^{14}C implies an unusually small value of the β-decay matrix element $(x\alpha - y\beta/\sqrt{3}) = (8.3 \pm 0.6)\times 10^{-4}$. This is hindered relative to other allowed Gamow-Teller transitions by approximately 5 orders of magnitude. This accidental cancellation of the β-decay matrix element imposes a strong constraint on possible ^{14}C and ^{14}N ground-state wave functions. This in turn has provided a good opportunity to test models of the nuclear force. The customary procedure has been to choose a particular form (usually the sum of a central plus tensor potential) for the nuclear potential,

to parametrize this potential in an empirical or semiempirical way, and to calculate α, β, γ, x, y. The results are then used to calculate the β-decay matrix element and the ground-state magnetic dipole and electric quadrupole moments of ^{14}N. The magnitude of the tensor force is varied with respect to the central force until cancellation of the β-decay matrix element occurs. Comparison of the other calculated properties with experiment then serves as a test of the theory for the potential.

Rose, Häusser, and Warburton[8] have reviewed the β- and γ-decay data in mass-14 nuclei. They concluded that cancellation of the β-decay matrix element is due primarily to a tensor force within an s^4p^{10} configuration. A small admixture of s^4p^8 ($2s$ and/or $1d$)^2, on the order of 10%, gave even better agreement with experiment.

C. Application of present results

In principle, by using the inelastic scattering cross section for the 2.313-MeV state, the ^{14}N and ^{14}C ground-state wave functions can be determined (within the framework of the present model) without recourse to the γ- and β-decay data. However, the 2.313-MeV state is weakly excited, and the present experiment does not supply enough information for this independent determination of the wave functions. In keeping with past theoretical work, the present data were interpreted in terms of the dominant s^4p^{10} configuration and fitted with the two parameters A_1 and (B_1-A_1) of Eq. (16b), as illustrated in Fig. 5. For this fit the form factors were converted back to Born approximation by a phase-shift calculation of the Coulomb distortion for magnetic transitions.[30] The harmonic-oscillator parameter a was fixed at the elastic scattering value, 1.68 fm.[22] The results of the linear least-squares fit to Eq. (16b) are

$$A_1 = 0.40 \pm 0.06,$$

$$B_1 - A_1 = 1.75 \pm 0.15.$$

Using this value of A_1, the reduced transition strength is calculated to be $B(M1, \omega)\uparrow = (4.3 \pm 1.3) \times 10^{-4}\ e^2\,\mathrm{fm}^2$. This result is larger than γ-decay measurements of this quantity, which average $(2.1 \pm 0.3) \times 10^{-4}\ e^2\,\mathrm{fm}^2$.[31,32] The difference may be due to the fact that in the present experiment A_1 must be obtained by extrapolation of the fit to lower q.

Because of the form of the associated radial integrals, A_1 is the dominant coefficient at low q (A_1 alone determines the radiative width) and (B_1-A_1) is the dominant coefficient at high q. The spin part of A_1 [the first term in Eq. (17)] is identical to the nearly vanishing β-decay matrix element. For this reason the radiative strength of the 2.313-MeV state and the low-energy electron scattering cross section are unusually small, and are dominated by the orbital part of A_1 [the second term in Eq. (17)].

Since the spin part of A_1 nearly vanishes, Eqs. (17) and (18) can be combined to yield

$$B_1 - A_1 \approx 4.71 \left\{ x\gamma/\sqrt{5} + y\beta/2\sqrt{3} + y\gamma 3\sqrt{2}/4\sqrt{5} \right\}. \tag{19}$$

Since the present experiment measures $B_1 - A_1$ with a smaller relative error than it measures A_1, and since the result for A_1 does not agree well with the γ-decay measurement at $q = \omega$, the

TABLE III. Configuration amplitudes for the wave functions for $T = 0$ and $T = 1$ ground states in mass-14 nuclei.

			Reference							
Coupling	T	Configuration	33	4	5	6	8	34	35	Present work
$L-S$	0	$\lvert {}^3S_1\rangle$	···	0.264	0.77	0.173	0.192	0.257	0.33	0.403
	0	$\lvert {}^1P_1\rangle$	···	0.374	0.179	0.355	0.471	0.544	0.41	−0.068
	0	$\lvert {}^3D_1\rangle$	···	0.89	0.981	0.920	0.861	0.800	0.85	0.913
	1	$\lvert {}^1S_0\rangle$	···	0.65	0.805	0.764	0.577	0.769	···	−0.093
	1	$\lvert {}^3P_0\rangle$	···	0.76	0.593	0.646	0.817	0.639	···	0.995
$j-j$	0	$\lvert \frac{1}{2}\frac{1}{2}1\rangle$	···	0.892	0.914	0.926	0.926	0.896	0.87	0.676
	0	$\lvert \frac{1}{2}\frac{3}{2}1\rangle$	···	0.410	0.397	0.362	0.296	0.286	0.37	0.735
	0	$\lvert \frac{3}{2}\frac{3}{2}1\rangle$	···	0.197	−0.087	0.119	0.234	0.344	0.28	−0.054
	1	$\lvert \frac{1}{2}\frac{1}{2}0\rangle$	···	0.99	0.949	0.967	1.000	0.966	···	0.760
	1	$\lvert \frac{3}{2}\frac{3}{2}0\rangle$	···	0.09	0.315	0.250	0.000	0.259	···	−0.651
Mean life × 10^{15} sec [a]			73 ± 18	26	43.8	28.8	8.2	13	···	75 ± 2
μ/μ_N			0.403 61	0.38	0.320	0.351	0.37	0.404 [b]	0.404 [b]	0.404 [b]
Q (mb)			16 ± 7	11	12	10.6	8.4	7.1 [b]	···	17.4 ± 0.2

[a] 2.313-MeV ($T = 1$) state in ^{14}N.

[b] Assumed known and used as a constraint.

magnitude of the form factor at higher q as given by $(B_1 - A_1)$ will be considered the primary result of this part of the experiment.

In principle, it would be possible to use only the electron scattering results [Eqs. (17) and (18)], the near-vanishing of the β-decay matrix element [Eq. (12)], and the normalization conditions to determine the five unknowns in Eqs. (10) and (11). However, as indicated the the preceding paragraph, the present determination of A_1 is suspect. The experimental value of the magnetic dipole moment of the ground state of ^{14}N is very accurate. Therefore, Eq. (13) was used as a constraint instead of Eq. (17). The simultaneous solution of the five equations (10)–(13) and (19) yields values of α, β, γ, x, and y as given in Table III. This table also presents determinations of these same quantities by other workers.[4-6,8,33-35]

As can be seen from Table III there is generally fair agreement among the various previous determinations of the strengths of the different configurations in the ground states of ^{14}N and ^{14}C. Some discrepancy is very likely due to the fact that not all possible shell-model configurations have been included in the space of the basis set. Different workers have in general used different sets of experimental data in extracting the configuration amplitudes, and these measured quantities may depend in varying degrees on the admixtures of higher configurations that have been neglected. Therefore, some lack of agreement among the various workers is probably not surprising. However, the values extracted from the present experiment are in qualitative disagreement with the previous determinations.

It is now possible to use the derived values of the amplitudes of the various configurations to make independent calculations of the quadrupole moment and the lifetime of the $T=1$ state, since Eqs. (14) and (15) were not used as constraints. The quadrupole moment of ^{14}N as calculated from Eq. (14) is 17.4 ± 0.2 mb. This is in very good agreement with the value of 16 ± 7 mb by Lin[36] from the magnetic resonance spectrum of NO, and with the most recent theoretical calculation of 19 mb by Freed and Ostrander.[37] Dally, Croissiaux, and Schweitz[22] derived a moment of 15.2 ± 4.2 mb from elastic electron scattering, again in good agreement with the present results. On the basis of earlier electron scattering data, Pal[38] and Fallieros and Ferrell[39] had concluded that a consistent fit of the electron scattering data and β-decay matrix element required a quadrupole moment of 30.7 mb, which in turn required a spheroidal deformation of ^{14}N ground-state charge distribution. However, the present inelastic electron scattering results are consistent with both the **elastic** electron scattering and the β decay without invoking deformation.

The lifetime of the 2.313-MeV ($T=1$) state in ^{14}N as calculated from Eq. (15) is $(75 \pm 2) \times 10^{-15}$ sec, in good agreement with γ-decay measurements. This agreement is probably even more significant than the agreement with measured values of the quadrupole moment because the radiative width of the state is more sensitive to the choice of configuration amplitudes than the quadrupole moment. However, the agreement on the radiative lifetime may be somewhat fortuitous, since small admixtures of higher configurations have not been considered.

V. 3.945-MeV ($T=1$) LEVEL

The present results for the form factors for this level are shown in Fig. 6 along with the results of Bishop, Bernheim, and Kossanyi-Demay.[9] The excitation of this level is a mixture of $C2$ and $M1$, but both of these experiments were sensitive only to the $C2$ (longitudinal) **part.** The results of Ref. 9 were fitted with the form factor

$$\langle 1p | j_1(qr) | 1p \rangle = xe^{-x} , \tag{20a}$$

where

$$x = \tfrac{1}{4} q^2 a^2, \qquad a = 1.68 \text{ fm}. \tag{20b}$$

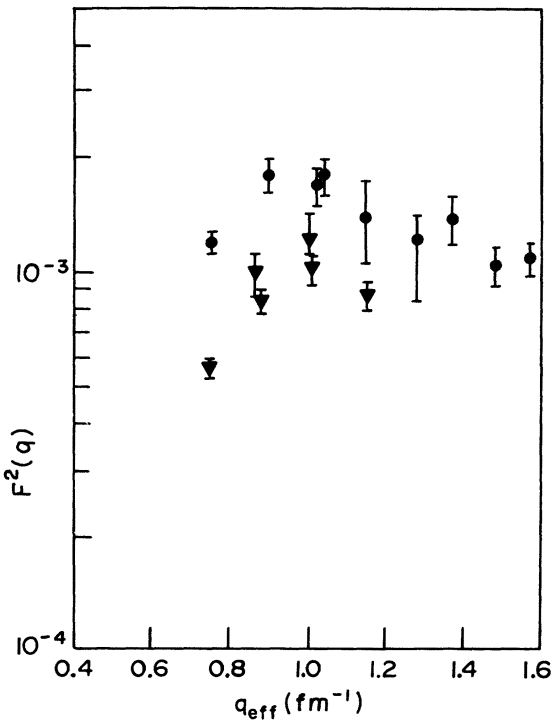

FIG. 6. A comparison of the present data (▼) and the data of Ref. 9 (●) for the 3.945-MeV (1^+) state in ^{14}N.

This form factor was based on a configuration assignment[40] of s^4p^{10} and resulted in a transition strength $B(C2, \omega)\uparrow = 6.2 \pm 0.4\ e^2\,\mathrm{fm}^4$.

The present results were fitted to the form factor

$$F(q_{\mathrm{eff}}) = x_{\mathrm{eff}} \exp[-(x_{\mathrm{eff}} + d)], \tag{21}$$

where q_{eff} and d have been previously defined and x_{eff} is calculated as in Eq. (20b) with q_{eff} substituted for q. This calculation resulted in a transition strength $B(C2, \omega)\uparrow = 3.4 \pm 0.3\ e^2\,\mathrm{fm}^4$.

The transition strength measured in the present experiment is a factor of 2 lower than that derived from the data of Ref. 9. This is to be expected from the experimental data since the present results are approximately a factor of 2 lower than those of Ref. 9. The source of this descrepancy is not known.

The present result for the transition strength is in fair agreement with the value of $2.6 \pm 0.3\ e^2\,\mathrm{fm}^4$ measured by Bister *et al.*[32] in a Doppler-shift-attenuation experiment. Olness, Poletti, and Warburton[41] have measured a value of $-(2.80 \pm 0.27)$ for the $E2/M1$ mixing ratio for this level. This number along with the present data would imply $B(M1, \omega)\uparrow = (5.0 \pm 0.7) \times 10^{-6}\ e^2\,\mathrm{fm}^2$.

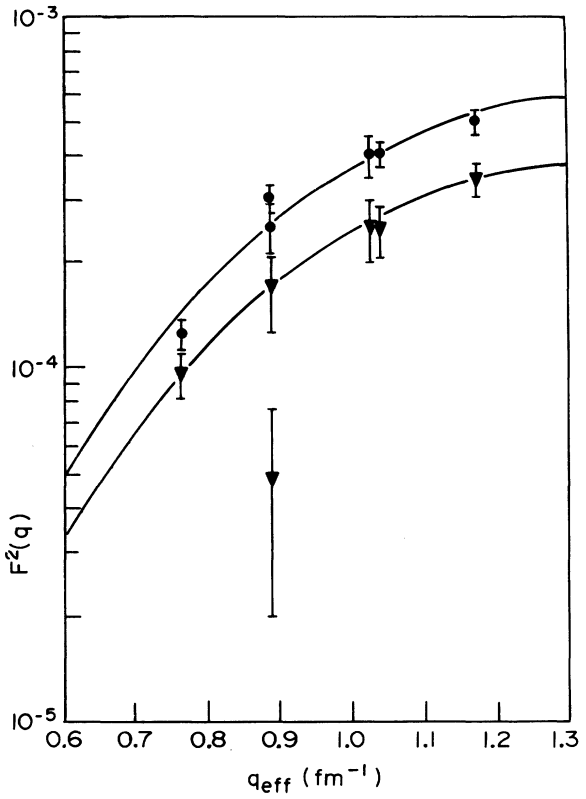

FIG. 7. Form factors squared of the 4.913-MeV (0^-) (triangles) and 5.106-MeV (2^-) (circles) states in ^{14}N. In both cases the fitted shape is that of Eq. (24) with $a = 1.82$ and 1.81 fm, respectively.

VI. INTERPRETATION OF THE NEGATIVE-PARITY LEVELS IN ^{14}N

A. Experimental observations

In the region of 5–6 MeV excitation, two groups of three peaks were observed in this experiment, as illustrated in Fig. 3. These peaks are the 4.43-MeV(2^+)^{12}C, 4.913-MeV(0^-)^{14}N, 5.106-MeV (2^-)^{14}N, and the 5.69-MeV(1^-)^{14}N, 5.83-MeV(3^-)^{14}N, 6.131-MeV(3^-)^{16}O levels. The squared form factors for the four ^{14}N peaks are illustrated in Figs. 7 and 8. The least-squares fits to the data described below typically yielded a χ^2 per degree of freedom of about 1.0.

The form factors of the weaker members of each doublet, the 4.913 MeV(0^-) and 5.69 MeV(1^-), show the same q dependence as the stronger 5.106-MeV(2^-) and 5.83-MeV(3^-) states. On the basis of the known spins and parities the lowest allowed multipolarities are ($C1$, $E1$), ($C1$, $E1$, $M2$), ($C1$, $E1$, $M2$, $C3$, $E3$), and ($C3$, $E3$, $M2$), respectively. The transverse parts are estimated to contain less

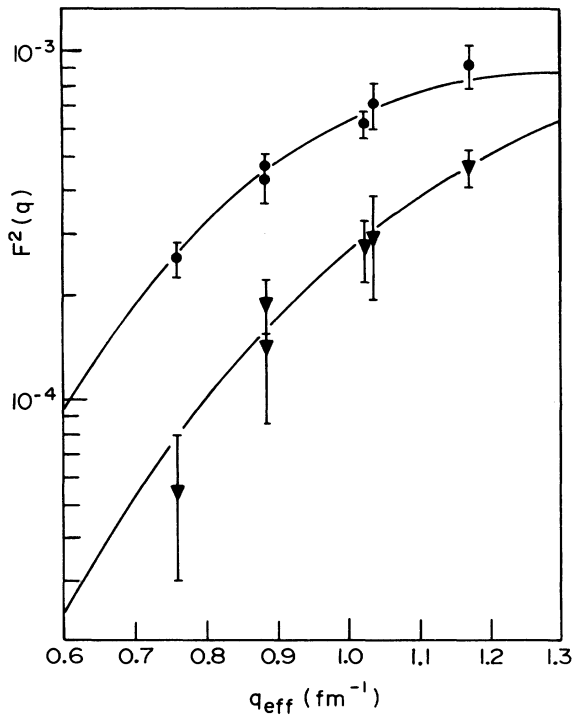

FIG. 8. Form factors squared of the 5.69-MeV (1^-) (triangles) and 5.83-MeV (3^-) (circles) states in ^{14}N. The fitted shape is that of Eq. (24) with $a = 1.37$ and 1.93 fm, respectively.

than 5% of the strength.[9] In fact, there is no experimental evidence in the present data for transverse excitation. All four excitations behave like $C3$ transitions because nuclear isospin selection rules forbid $C1$, $T=0$ to $T=0$ transitions in self-conjugate nuclei. More precisely, the first term in the $C1$ matrix element, which is proportional to $\langle J_f || qr || J_i \rangle$, vanishes under these conditions. Then the leading term for both $C1$ and $C3$ transitions is proportional to q^3. The present data were taken at $qr \leq 2$, below the first maximum of the form factors. Under these conditions the electron scattering cross sections for all four negative-parity states can be expected to approximate a q^6 dependence on momentum transfer.

B. Theoretical interpretation

Scattering of electrons and nucleons from ^{14}N and radiative decays in ^{14}N have usually been interpreted in terms of the individual particle shell model. Comprehensive calculations of energies, spins, and parities of states up to 10–12 MeV have been carried out by Talmi and Unna,[42] Warburton and Pinkston,[40] True,[43] Sebe,[44] Hsieh and Horie,[45] and Jäger, Kissener, and Eramzhian.[46] A consistent feature of the shell-model calculations is the assumption of an inert ^{12}C core, $1s^4\ 1p^8$. The four lowest negative-parity states are then considered to be the result of exciting one of the two $1p_{1/2}$ particles to the nearly degenerate $2s_{1/2}$ and $1d_{5/2}$ shells. The configurations shown in Table IV are found to be the dominant ones. The various shell-model calculations find amplitudes of 0.92 to 0.99 for these dominant configurations.

Also shown in Table IV are the transition strengths predicted by some of the calculations. Warburton and Pinkston[40] assumed extreme jj coupling and effective charges of 1.1 for the neutron and 2.1 for the proton. This leads to a collective enhancement by a factor of 10 for the transition rates. Smaller strengths can be derived from the model of Lane.[46,47] Here the lowest negative-parity states are considered due to the weak coupling of a $2s_{1/2}$ or $1d_{5/2}$ proton to ^{13}C. A coupling to the $(1/2^-)$ ^{13}C ground state yields four $T=0$ states of spin 0^-, 1^-, 2^-, 3^- in the 5–6-MeV region and four $T=1$ states in the 8–10-MeV region. These states should have single-particle reduced widths since ^{13}C is the unique parent. Jäger, Kissener, and Eramzhian[46] used harmonic-oscillator wave functions and calculated all $1\hbar\omega$ configurations in intermediate coupling. No effective charge was assumed and the harmonic-oscillator parameter of 1.7 fm was taken from elastic electron scattering. Shell spacings and force parameters were adjusted to fit energy levels in other $1p$ nuclei. The positions of the lowest 17 levels in ^{14}N were calculated correctly to within 0.7 MeV.

Another matter of interest is the amount of isotopic spin impurity in these $T=0$ states. Warburton and Pinkston[40] estimate that a 5% $T=1$ impurity gives the best agreement with experiment. True[43] and Hsieh and Horie[45] estimate 1% or less. In the model of Lane[47] these impurities can be due to mixing between the four $T=0$ and the four $T=1$ negative-parity states based on the ground state of ^{13}C. Recently Renan *et al.*[48] measured a 9% $T=1$ impurity in the 5.69-MeV $T=0$ level and 5% $T=0$ impurity in the 8.06-MeV $T=1$ level.

For the four negative-parity states, the above literature does not provide any wave functions from which electron scattering cross sections can be directly calculated. In the absence of these, the present data were interpreted in the following way: (1) The shapes of the form factors were compared to the results expected on the basis of pure $1p_{1/2}$, $2s_{1/2}$ and $1p_{1/2}$, $1d_{5/2}$ configurations.

TABLE IV. Transition strengths for the lowest negative-parity states in ^{14}N.

	Transition strength in single-particle units								
	Theoretical values				Experimental values				
Level	Dominant configuration	Ref. 42	Ref. 46	Ref. 47	Present[a] work	Ref. 9[a]	Ref. 51[b]	Ref. 52[b]	Ref. 53[b]
4.913(0^-)	$(1s_{1/2})^4\ (1p_{3/2})^8$ $(1p_{1/2})\ (2s_{1/2})$	...	...	...	$(1.1\pm0.5)\times10^{-7}$	...	...	...	...
5.106(2^-)	$(1s_{1/2})^4\ (1p_{3/2})^8$ $(1p_{1/2})\ (1d_{5/2})$	10	5.2	1.0	4.1 ± 1.3	8.9 ± 0.9	1.6–6.8	2.2 ± 0.7	2.1 ± 0.5
5.69(1^-)	$(1s_{1/2})^4\ (1p_{3/2})^8$ $(1p_{1/2})\ (2s_{1/2})$	...	0.0062	...	$(3.8\pm2.1)\times10^{-8}$	...	...	...	...
5.83(3^-)	$(1s_{1/2})^4\ (1p_{3/2})^8$ $(1p_{1/2})\ (1d_{5/2})$	10	2.4	1.0	6.1 ± 1.3	9.3 ± 0.5	<12.3	1.1–11.5	...

[a] Measurement by inelastic electron scattering.
[b] Measurement by γ-ray decay using Doppler-shift-attenuation method.

(2) A two-parameter fit to the data

$$|\psi\rangle = \xi|T=0\rangle + \eta|T=1\rangle \tag{22}$$

was made to extract $T=1$ components. (3) The cross sections were extrapolated to $q^2=\omega^2$ to compare single-particle strengths with the models described above.

C. Interpretation of present experimental results

For the configurations of Table IV, the form factors calculated for the shell model with harmonic-oscillator wave functions are[26]

$$F_{C1}(q^2) \sim \langle 1p|j_1(qr)|1d\rangle\, e^{-d} = \tfrac{1}{3}(10x)^{1/2}(1-\tfrac{2}{5}x)e^{-(x+d)}, \tag{23a}$$

$$F_{C1}(q^2) \sim \langle 1p|j_1(qr)|2s\rangle\, e^{-d} = \tfrac{2}{3}(x)^{1/2}(1-x)e^{-(x+d)}, \tag{23b}$$

$$F_{C3}(q^2) \sim \langle 1p|j_3(qr)|1d\rangle\, e^{-d} = \tfrac{2}{3}(\tfrac{2}{5})^{1/2}x^{3/2}e^{-(x+d)}. \tag{23c}$$

After the $C1$ form factors are corrected for the vanishing term $\langle J_f|qr|J_i\rangle$, all four transitions are of the form

$$F(q^2) \sim x^{3/2}e^{-(x+d)}. \tag{24}$$

The fits of these shell-model functions to the data are illustrated in Figs. 7 and 8 and the transition probabilities extracted from the fits are included in Table IV. The oscillator parameter a was allowed to vary from the value used to fit the elastic scattering in order to get a best fit to the shape of the form factor.

In order to test the sensitivity of the data to a particular model for the nuclear charge distribution, the data were also fitted to the Helm[49] model,

$$F_{CL}(q^2) = j_L(qR)e^{-g^2q^2/2}. \tag{25}$$

In this model the radial dependence of the transition charge is assumed to be given by a spherical shell of Gaussian form centered at a radius R. This radius was allowed to vary from the ground-state r.m.s. radius to get a best fit. The width of the Gaussian is determined by g, here chosen to be 1.02 fm, a value obtained in fitting ^{12}C data.[50] However, when g was allowed to vary the result was 1.02 ± 0.02, and the fits were not significantly altered. The χ^2's, reduced transition probabilities, and shapes of the function for the shell-model fits are practically identical to those for the Helm-model fits.

An attempt to estimate $T=1$ impurities by a fit to Eq. (22) was unsuccessful because the shapes of the form factors are not known with sufficient accuracy. The radiative strength is due primarily to the $T=1$ admixture, while the electron scattering is primarily sensitive to the $T=0$ component. Therefore, the unknown lifetimes of the 4.913- and 5.69-MeV levels cannot be extracted from the electron scattering data. However, upper limits on the lifetimes have been obtained from Doppler-shift-attenuation measurements.[51] These lifetimes are much shorter than those which could be derived from the present data if the wave functions were pure $T=0$. Thus the radiative strengths are due primarily to the $T=1$ impurities. The impurities of the 4.913- and 5.69-MeV levels can then be estimated to be $\geq 2\%$ by comparison with the upper limits on the lifetimes.

The 5.106 (2^-) transition to the ground state is a mixture of $C1$ and $C3$. A mixing ratio of $C3/C1 = 0.15\pm0.025$ is reported by Allen, Alexander, and Healey.[52] The present experiment cannot distinguish between the actual $C3$ component and the $C3$ behavior of the forbidden $C1$ component. However, the former will provide almost all of the measured radiative strength. Because of the $C3$ component, the isospin impurity cannot be extracted by the method described above. This

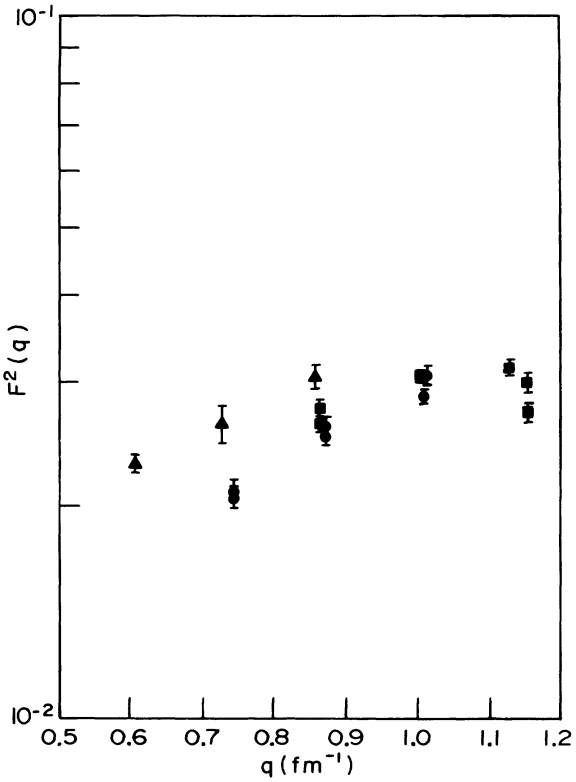

FIG. 9. Form factor squared of the 2.429-MeV ($\frac{5}{2}^-$) state in ^{9}Be. The data are shown before the separation into transverse and longitudinal parts was carried out: ▲— data taken at 163°, ■— data taken at 145°, ●— data taken at 110°.

TABLE V. Electron scattering form factors for ^{9}Be.

Energy (MeV)	Angle (deg)	q [a] (fm^{-1})	$F^2(q)$ elastic [b]	$F^2(q)\times 10^3$ 2.429-MeV level Be_3N_2 target	$F^2(q)\times 10^3$ 2.429-MeV level Be metal target
60.65	163.66	0.604	0.4885	22.9±0.6	
73.06	163.44	0.727	0.3447	26.1±1.7	
89.82	110.79	0.744	0.3257	20.8±0.9	20.6±0.7
86.31	163.44	0.857	0.2207	30.5±1.2	
90.08	145.92	0.865	0.2144	27.4±0.4	
				26.1±0.7	
104.95	110.79	0.868	0.2118	25.8±0.9	24.9±0.5
104.62	145.71	1.002	0.1218	30.4±0.5	30.5±0.4
122.00	110.51	1.006	0.1202	30.6±1.0	28.5±0.6
117.62	145.65	1.125	0.0676	31.2±0.7	
120.01	145.97	1.148	0.0598	29.8±0.9	27.0±0.8

[a] Calculated for elastic scattering.
[b] Calculated from the parameters of Ref. 56.

method is also inapplicable to the 5.83(3^-) transition to the ground state, whose longitudinal part is pure $C3$.

Table IV compares the present results for the 5.106- and 5.83-MeV transitions with earlier electron scattering results (Ref. 9) and with other methods. In general, the present results are in agreement with the γ-decay measurements. The present value for the 5.106-MeV strength is close to that calculated by Jäger, Kissener, and Eramzhian,[46] but the present 5.83-MeV strength is in disagreement with the same calculations.

VII. 2.429-MeV ($\frac{5^-}{2}$) ^{9}Be LEVEL

Since runs on ^{9}Be were necessary to obtain the net ^{14}N scattering from the Be_3N_2 target, data were also obtained on the inelastic scattering of electrons from the second excited state in ^{9}Be. As in the case of ^{14}N, the inelastic form factors were extracted by comparison of the area of the 2.429-MeV level to that of the ^{9}Be elastic peak. The calculated elastic and measured inelastic form factors are given in Table V and illustrated in Fig. 9. This level has also been studied in previous experiments for example by Nguyen Ngoc, Hors, and Perez-y-Jorba,[54] by Vanpraet and Barber,[55] and by Clerc, Wetzel, and Spamer.[56] The present data were interpreted by the same model used by the above workers except that the "effective q" approximation [Eq. (5)] was used instead of the 4% correction employed by Clerc, Wetzel, and Spamer.[56]

An attempt was made to separate the data into longitudinal and transverse parts according to Eq. (4). However, the uncertainties in the transverse form factors were so large that a meaningful value of $B(M1,\omega)\uparrow$ could not be extracted. The analysis of the present data yielded a value of $B(C2,\omega)\uparrow$ of $45.7\pm3.5\ e^2\,fm^4$ for this level. This is to be compared with the values $52.2\pm2.0\ e^2\,fm^4$ reported in Ref. 54 and $41.6\pm2.9\ e^2\,fm^4$ reported in Ref. 56. Thus, the present data appear to be in fair agreement with previous measurements.

VIII. CONCLUSIONS

The measured form factors for the 2.313-MeV ($T=1$) transition have been used as constraints on the ^{14}N and ^{14}C ground-state wave functions. Within the framework of the shell-model configurations included in the calculations these wave functions have been determined with good precision. In the LS representation the triplet states appear to dominate in the ground-state wave functions of ^{14}C and ^{14}N. The ground-state quadrupole moment and lifetime of the 2.313-MeV state in ^{14}N are accurately predicted by the present wave functions.

The form factors for the negative-parity states were not determined with sufficient precision to allow direct extraction of the $T=1$ admixture. This is because the electron scattering is primarily sensitive to the dominant $T=0$ component of the wave functions. However, in the case of the 4.91- and 5.69-MeV levels, which are almost entirely $C1$ excitations, a lower limit of 2% can be set for the relative intensity of the $T=1$ admixture.

ACKNOWLEDGMENTS

We would like to thank G. Rawitscher for providing the phase-shift code for elastic scattering, and B. Chertok for providing the corrections for inelastic scattering. We are grateful to J. Berg-

strom for the use of his data reduction programs and for many helpful discussions. We are especially grateful to D. Peaslee for communicating to us his results on the calculation of the $M1$ matrix elements and for numerous stimulating conversations.

---

†Work supported in part by the U. S. Atomic Energy Commission, Contract No. AT(11-1)-3069.

*Present address: U. S. Naval Research Laboratory, Washington, D. C.

[1]D. R, Inglis, Rev. Mod. Phys. 25, 390 (1953).
[2]E. Baranger and S. Meshkov, Phys. Rev. Lett. 1, 30 (1958).
[3]H. A. Weidenmüller, Nucl. Phys. 36, 151 (1962).
[4]B. Jancovici and I. Talmi, Phys. Rev. 95, 289 (1954).
[5]J. P. Elliot, Phil. Mag. 1, 503 (1956).
[6]W. M. Visscher and R. A. Ferrell, Phys. Rev. 107, 781 (1957).
[7]L. Zamick, Phys. Lett. 21, 194 (1966).
[8]H. J. Rose, O. Häusser, and E. K. Warburton, Rev. Mod. Phys. 40, 591 (1968).
[9]G. R. Bishop, M. Bernheim, and P. Kossanyi-Demay, Nucl. Phys. 54, 353 (1964).
[10]J. E. Leiss, Los Alamos Scientific Laboratory Report No. LA3609, 1966 (unpublished), p. 20; S. Penner, National Bureau of Standards Technical Note No. 523, 1970 (unpublished).
[11]J. S. Pruitt, Nucl. Instrum. Methods 100, 433 (1972).
[12]S. Penner and J. W. Lightbody, Jr., in *Proceedings of the International Symposium on Magnet Technology, Stanford, California, 1965*, edited by H. Brechna and H. S. Gordon (Stanford Linear Accelerator Center, 1965), p. 154. Available from Clearinghouse for Federal, Scientific, and Technical Information, Springfield, Va.
[13]J. W. Lightbody, Jr., and S. Penner, IEEE Trans. Nucl. Sci. NS-15, 419 (1968).
[14]X. K. Maruyama and J. C. Bergstrom, National Bureau of Standards Internal Report No. 297, 1969 (unpublished).
[15]S. Penner, National Bureau of Standards Internal Report No. 302, 1969 (unpublished).
[16]H. Nguyen Ngoc and J. Perez-y-Jorba, Phys. Rev. B136, 1036 (1964).
[17]J. Bergstrom, in Massachusetts Institute of Technology 1967 Summer Study, U. S. Atomic Energy Commission Report No. TID-24667, 1967 (unpublished), p. 251.
[18]J. W. Lightbody, Jr., Ph. D. thesis, University of Maryland, 1970 (unpublished).
[19]S P. Fivozinsky, Ph. D. thesis, University of Connecticut, 1971 (unpublished).
[20]W. G. Davies, private communication.
[21]P. R. Bevington, *Data Reduction and Error Analysis for the Physical Sciences* (McGraw-Hill, New York, 1919), p. 243.
[22]E. B. Dally, M. G. Croissiaux, and B. Schweitz, Phys. Rev. 188, 1590 (1969).
[23]H. A. Bentz, Z. Naturforsch. 24a, 858 (1969).
[24]H. Uberall, *Electron Scattering from Complex Nuclei* (Academic, New York, 1971), Part A, pp. 162 and 170.
[25]G. Bishop, private communication.
[26]R. S. Willey, Nucl. Phys. 40, 529 (1963).
[27]L. J. Tassie and F. C. Barker, Phys. Rev. 111, 940 (1958).
[28]T. deForest, Jr., and J. D. Walecka, Adv. Phys. 15, 1 (1966).
[29]D. Peaslee, private communication.
[30]B. T. Chertok, Phys. Rev. 187, 1340 (1969).
[31]S. J. Skorka, J. Hertel, and T. W. Retz-Schmidt, Nucl. Data A2, 347 (1966).
[32]M. Bister, A. Anttila, M. Piiparinen, and M. Viitasalo, Phys. Rev. C 3, 1972 (1971).
[33]F. Ajzenberg-Selove, Nucl. Phys. A152, 1 (1970).
[34]R. Sherr, J. B. Gerhart, H. Horie, and W. F. Hornyak, Phys. Rev. 100, 945 (1955).
[35]S. Varma and P. Goldhammer, Nucl. Phys. A125, 193 (1969).
[36]C. A. Lin, Phys. Rev. 119, 1027 (1960).
[37]N. Freed and P. Ostrander, Nucl. Phys. A111, 63 (1968).
[38]M. K. Pal, Phys. Rev. 117, 566 (1960).
[39]S. Fallieros and R. A. Ferrell, Phys. Rev. 116, 660 (1959).
[40]E. K. Warburton and W. T. Pinkston, Phys. Rev. 118, 733 (1960).
[41]J. W. Olness, A. R. Poletti, and E. K. Warburton, Phys. Rev. 154, 971 (1967).
[42]I. Talmi and I. Unna, Annu. Rev. Nucl. Sci. 10, 353 (1961).
[43]W. True, Phys. Rev. 130, 1530 (1965).
[44]T. Sebe, Prog. Theor. Phys. 30, 290 (1963).
[45]S. T. Hsieh and H. Horie, Nucl. Phys. A151, 243 (1970).
[46]H. U. Jäger, H. R. Kissener, and R. A. Eramzhian, Nucl. Phys. A171, 16 (1971).
[47]A. M. Lane, Massachusetts Institute of Technology Report, 1955 (unpublished).
[48]M. J. Renan, J. P. Sellschop, R. J. Keddy, and D. W. Mingay, Nucl. Phys. A193, 470 (1972).
[49]R. H. Helm, Phys. Rev. 104, 1466 (1956).
[50]M. Rosen, R. Raphael, and H. Uberall, Phys. Rev. 163, 927 (1967).
[51]K. P. Lieb and R. Hartmann, Z. Phys. 200, 432 (1967).
[52]K. W. Allen, T. K. Alexander, and D. C. Healey, Can. J. Phys. 46, 1575 (1968).
[53]G. Meyer, Professional Commission on Nuclear Physics, Bad Neunahr, Germany, CONF-680461-9, 1968 (unpublished).
[54]H. Nguyen Ngoc. M. Hors, and J. Perez-y-Jorba, Nucl. Phys. 42, 62 (1963).
[55]G. J. Vanpraet and W. C. Barber, Z. Phys. 211, 213 (1968).
[56]H. G. Clerc, K. J. Wetzel, and E. Spamer, Nucl. Phys. A120, 441 (1968).